JACS
JOURNAL OF THE AMERICAN CHEMICAL SOCIETY
Article
pubs.acs.org/JACS

Effector Roles of Putidaredoxin on Cytochrome P450cam Conformational States

Shu-Hao Liou, Mavish Mahomed,[†] Young-Tae Lee,[‡] and David B. Goodin*

Department of Chemistry, University of California, Davis, One Shields Avenue, Davis, California 95616, United States

Supporting Information

ABSTRACT: In this study, the effector role of Pdx (putidaredoxin) on cytochrome P450cam conformation is refined by attaching two different spin labels, MTSL or BSL (bifunctional spin-label) onto the F or G helices and using DEER (double electron−electron resonance) to measure the distance between labels. Recent EPR and crystallographic studies have observed that oxidized Pdx induces substrate-bound P450cam to change from the closed to the open state. However, this change was not observed by DEER in the reduced Pdx complex with carbon-monoxide-bound P450cam ($Fe^{2+}CO$). In addition, recent NMR studies have failed to observe a change in P450cam conformation upon binding Pdx. Hence, resolving these issues is important for a full understanding the effector role of Pdx. Here we show that oxidized Pdx induces camphor-bound P450cam to shift from the closed to the open conformation when labeled on either the F or G helices with MTSL. BSL at these sites can either narrow the distance distribution widths dramatically or alter the extent of the conformational change. In addition, we report DEER spectra on a mixed oxidation state containing oxidized Pdx and ferrous CO-bound P450cam, showing that P450cam remains closed. This indicates that CO binding to the heme prevents P450cam from opening, overriding the influence exerted by Pdx binding. Finally, we report the open form P450cam crystal structure with substrate bound, which suggests that crystal packing effects may prevent conformational conversion. Using multiple labeling approaches, DEER provides a unique perspective to resolve how the conformation of P450cam depends on Pdx and ligand states.

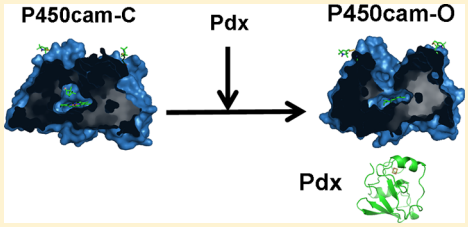

INTRODUCTION

Cytochromes P450 are heme-containing monooxygenases that utilize O_2 and reducing equivalents to catalyze oxygen insertion into a large variety of substrates ranging from bacteria to man.[1,2] The oxidation products are utilized in diverse pathways from drug metabolism to biosynthesis.[3,4] With over 30 000 members, the cytochromes P450 share a common fold and heme chemistry but differ greatly in specificity for substrate oxidation and in their requirements for electron source.[5−8] The most well understood P450cam, CYP101A1, from the soil bacterium *Pseudomonas putida* metabolizes camphor as substrate.[9−11] It is also unique in its requirement for a specific reductase, putidaredoxin (Pdx), as the electron source.[12,13] The reaction cycle begins with the heme in a low-spin ferric state which converts to the high-spin state when the enzyme binds substrate.[14−17] This allows reduction by the first electron from Pdx. The resulting ferrous enzyme binds O_2 before the second electron is delivered from Pdx to generate the ferric-hydroperoxo complex.[17−21] A crucial step in the cycle is the heterolytic cleavage of the peroxy bond to generate the reactive compound I intermediate responsible for substrate hydroxylation.[2,22,23] The first electron can be provided by Pdx or an external electron donor, but no biological reductant other than Pdx is effective for the second electron transfer.[24] In addition to its role as the electron donor, Pdx binding is known to induce changes in the structure and spectroscopic features of the enzyme.[25−30] However, the nature of this effector role has only recently begun to be better understood.

Early crystal structures of P450cam bound to camphor, product, ligands, or substrate-released forms were shown to be in a closed conformation,[9,10,31,32] although it was widely recognized that a more open structure must exist during the catalytic cycle at least to allow substrate binding and product release.[33−35] The observation of open conformations of the enzyme awaited more recent reports from crystals grown in the presence of large substrate analogues linked to reporter groups.[36−39] A study of 30 crystal structures of P450cam bound to such analogues revealed that the enzyme can adopt three distinct conformational substates: P450cam(C), P450cam(I), and P450cam(O) corresponding to the closed, intermediate, and open forms.[40] These states involve differential movements of the F and G helices that cover the substrate binding channel. A subsequent crystal structure showed substrate-free enzyme to be in the P450cam(O) state.[40,41] Double electron−electron resonance (DEER)[42,43] measurements of spin-labeled P450cam showed that, in solution, the substrate-free enzyme existed in the fully open conformation and converted to the closed state upon binding substrate.[43] These studies supported a view of P450cam function, in which its structure is characterized by conformational selection within a small set of distinct conformations, rather than being subject to a distribution of malleable, induced-fit states.[44]

Received: April 21, 2016
Published: July 25, 2016

DOI: 10.1021/jacs.6b04110
J. Am. Chem. Soc. 2016, 138, 10163−10172

Three reports in 2013 revealed new details about the effects of Pdx binding on the conformation of P450cam. A crystal structure of oxidized Pdx (Pdx_{ox}) covalently tethered to substrate-bound P450cam showed the enzyme in the fully open conformation,[45] and chemical reduction of the oxidized crystals did not alter this open conformation of the enzyme. An independent DEER study also showed that binding of Pdx_{ox} to the camphor-bound oxidized enzyme resulted in its conversion from the closed to the fully open conformation.[46] However, the DEER study showed that in solution, ferrous-CO P450cam, when bound to reduced Pdx (Pdx_{red}), remained in the closed conformation.[46] A crystal structure of an untethered complex between Pdx and substrate-free P450cam was also reported with the enzyme in the open conformation, but in this case, the open state was attributed to the absence of camphor rather than the influence of Pdx.[47] These results have been recently challenged by an NMR study of P450cam labeled on the G helix with a large paramagnetic complex.[48] This study concluded that oxidized substrate-bound ferric P450cam remains closed upon binding Pdx_{ox}. Thus, recent studies have resulted in very different conclusions about the effect of Pdx binding on the structure of P450cam.[45−50] This has left several very important questions unanswered about the effector role of Pdx on P450cam conformation. Does Pdx induce the change from closed-to-open in all oxidation and coordination states of the system? Is there evidence in solution for intermediate open conformations? How do the methods of crystallography, EPR, and NMR differ in reporting these changes? The crystallographic studies contain the most detailed description of the overall protein structure but are uncertain about the oxidation states due to the effects of in-beam reduction.[45] In addition, effects of crystal contacts on conformation are possible. The EPR approach allows study of samples in solution and with well-defined redox states,[43,46] but the experiments must be performed at cryogenic temperatures.[51] Finally, while the NMR experiments were performed at room temperature,[48] they employed covalent labeling with a large paramagnetic complex at two sites within the mobile G helix, and labeling may itself affect the delicate energetics of the conformational changes involved.

In this study, we report DEER data collected on complexes in a mixed oxidation state, and on states labeled at multiple sites within the F and G helices with both single- and bifunctional spin-labels (Figure 1). We also report X-ray crystallographic

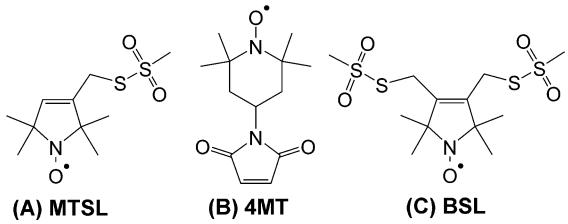

Figure 1. Three different spin labels applied in this report.

characterization showing nonspecific binding of camphor to the open conformation of the enzyme. These studies provide important new insights on the role of the oxidation and coordination state of the enzyme and the role played by Pdx in inducing these states.

RESULTS

Mixed Oxidation State Complex. In a previous study, we showed using DEER that binding of oxidized Pdx_{ox} to ferric substrate-bound P450cam ($P450cam(Fe^{3+}{\cdot}S)/Pdx_{ox}$) resulted in the conversion of the enzyme from the closed to the open conformation.[46] This was consistent with the observations of the tethered complex by X-ray crystallography,[45] and these two studies have provided the basis for a proposal that the long-known effector role of Pdx is to favor the open state of P450cam. However, the DEER data also indicated that when reduced Pdx_{red} binds to the ferrous-CO state of P450cam ($P450cam(Fe^{2+}CO{\cdot}S)/Pdx_{red}$), the enzyme remained in the closed conformation. As illustrated in Figure 2, this suggested

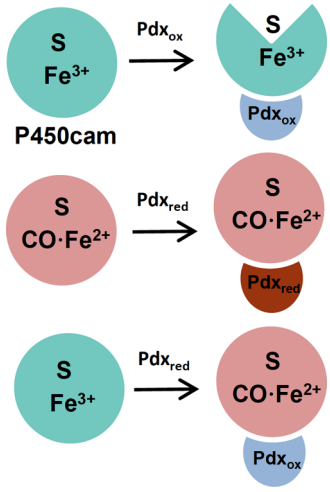

Figure 2. A cartoon depiction of the first hypothesis tested in this study, that CO coordination rather than redox state controls the conformational response to Pdx binding. The figure depicts the conformational state of P450cam (large circle represents closed, segmented circle represents open), whether it is bound by Pdx (small circle), and the coordination and oxidation state of the proteins (text labels). The oxidation state is also indicated by the color scheme (red/pink for reduced, blue/green for oxidized). The top panel summarizes our previous DEER studies[43,46] showing that Pdx binding to oxidized substrate-bound P450cam induces conversion to the open conformation. The second panel shows that this conversion does not occur when all proteins are reduced and the ferrous heme is coordinated by CO. The bottom panel shows the results expected from the hypothesis that it is CO coordination rather than protein redox state that controls whether the effector function of Pdx is allowed.

that the effector-driven conformational shift is either modulated by the redox state of Pdx or is otherwise opposed in the ferrous-CO state, which is not formed during native turnover. This result appears to differ from the crystallographic observations of Tripathi et al., where chemical reduction of the crystals of the tethered complex did not convert the enzyme to the closed conformation.[45] The different results obtained by the two studies could be due to the heme−CO coordination in the DEER experiments[52] and/or to the effects of crystal packing in the X-ray study.

To examine further whether the conformational shift depends on the redox state of Pdx or on the coordination state of P450cam (see Figure 2), we present DEER measurements on samples in the $P450cam(Fe^{2+}CO{\cdot}S)/Pdx_{ox}$ mixed oxidation state. A sample of ferric P450cam containing camphor, CO and labeled with MTSL at positions S190C and

DOI: 10.1021/jacs.6b04110
J. Am. Chem. Soc. 2016, 138, 10163−10172

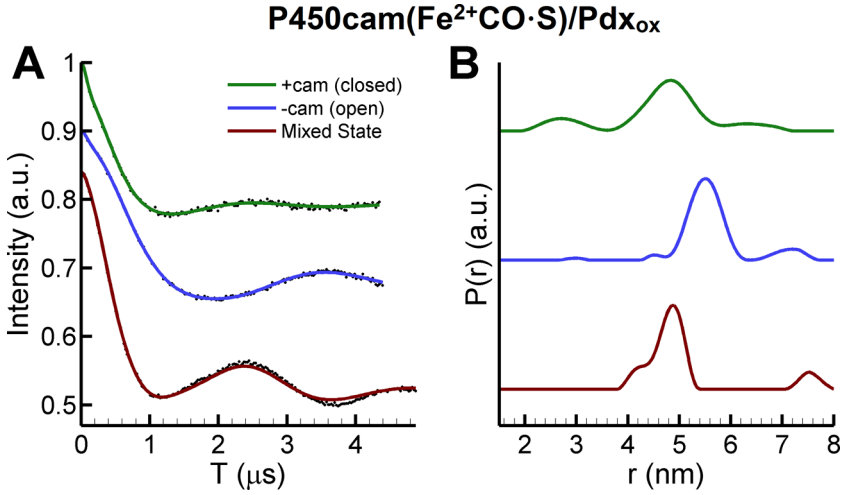

Figure 3. DEER spectra of the mixed oxidation state complex in which P450cam is in the ferrous-CO state and putidaredoxin is in the oxidized (Pdx_{ox}) state. (A) Time-domain spectra of P450cam DEER with two MTSL labels, placed on S190C and S48C in three different states: (green) camphor-bound, (blue) camphor-free, and (red) P450cam($Fe^{2+}CO{\cdot}S$)/Pdx_{ox}. Black points are the raw data after background subtraction,and the solid traces are the fitted curves. (B) Distance distributions obtained by Tikhonov regularization.[53]

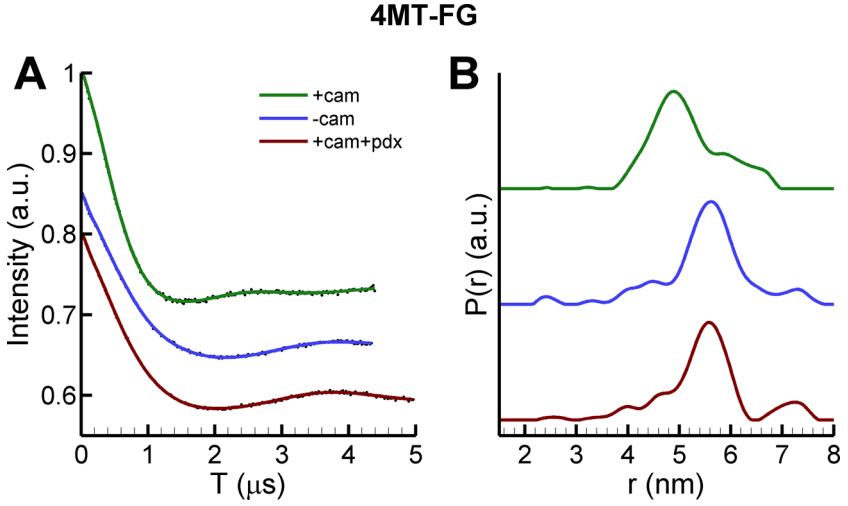

Figure 4. DEER spectra of the oxidized state complex in which P450cam is in the ferric state and putidaredoxin is also oxidized (Pdx_{ox}). P450cam contained two 4MT labels, placed on S190C and S48C in three different states: (green) camphor-bound, (blue) camphor-free, and (red) camphor and Pdx bound. (A) Time domain DEER spectrum: black points are the raw data after background subtraction, and the solid traces are the fitted curves. (B) Distance distributions obtained by Tikhonov regularization.[53]

S48C (Figure S1) was titrated with a quantity, determined experimentally (see Methods), of Pdx_{red} just sufficient to result in the stoichiometric reduction of the enzyme to give P450cam($Fe^{2+}CO{\cdot}S$)/Pdx_{ox}. The redox state and coordination of the mixed state were verified by UV/vis and CW EPR (see Figure S2). In Figure 3, the four-pulse Q-band DEER spectrum of P450cam($Fe^{2+}CO{\cdot}S$)/Pdx_{ox} complex is compared with reference samples of ferric P450cam prepared in the open substrate-free and closed substrate-bound conformations.[43] Upon conversion of the time domain spectra to distance distribution plots by Tikhonov regularization,[53] the P450cam-($Fe^{2+}CO{\cdot}S$)/Pdx_{ox} complex shows a single dominant distance (48.6 Å) that is in excellent agreement with that (48.4 Å) of the closed conformation and distinct from that (55.1 Å) of the open conformation. To confirm our previous observation that the oxidized state of the P450cam($Fe^{3+}{\cdot}S$)/Pdx_{ox} complex converts to the open conformation, we have performed DEER measurements on the protein labeled at positions S190C and S48C with 4-maleimido-TEMPO (4MT). This alternative to the MTSL spin-label used in the previous study was used to demonstrate that the conformational conversion is independent of the identity of the label.[54] Shown in Figure 4 are the DEER spectra for the open, closed, and P450cam($Fe^{3+}{\cdot}S$)/Pdx_{ox} complex showing that binding of Pdx_{ox} to the ferric P450cam converts it to a single species with a distance (55.8 Å) consistent with the open conformation. Thus, these data confirm that Pdx_{ox} binding converts substrate-bound ferric P450cam from the closed to the open state, but it fails to convert ferrous-CO P450cam from the closed conformation.

Bifunctional Spin-Labeling on the F and G Helices. Pairs of bifunctional spin-labels were introduced at a reference location and on either the F or G helix to examine in greater detail the segmental movements of these helices in the open, intermediate, and closed states (Figure 5). One of the problems with single-site attachment of spin-labels such as MTSL or 4MT is the rotamer distribution introduced by the flexible spin-

DOI: 10.1021/jacs.6b04110
J. Am. Chem. Soc. 2016, 138, 10163−10172

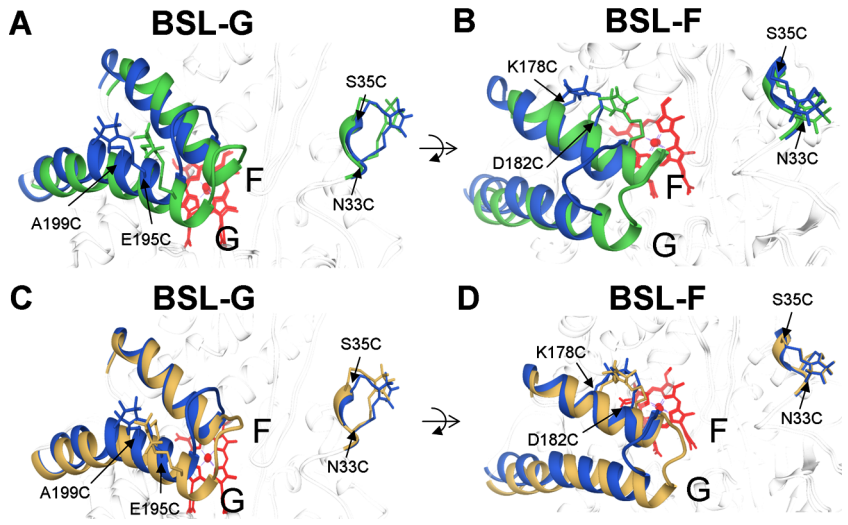

Figure 5. Models showing placement of BSL spin-labels to probe differential movement in the F and G helices. The models are based on the three conformational states known from crystal structures[41] for the open (blue), intermediate (yellow), and closed (green) states. For the labeled mutant BSL-G, shown in panels A and C, one fixed BSL bifunctional label is attached at N33C and S35C, and the label on the G helix is attached at A199C and E195C. For the labeled mutant BSL-F, shown in panels B and D, one fixed BSL bifunctional label is attached at N33C and S35C as before, and the label on the F helix is attached at K178C and D182C. See Table 1 for the label attachment key. The heme is shown in red. The orientation of all models is very similar, though a small rotation about the axis gnome shown was performed for B and D to allow the position of the F helix labels to be seen. Models for MTSL-F and MTSL-G are not shown for clarity but would include one of the two pairs shown above and in Table 1. Figures were made using UCSF Chimera.[55]

label, resulting in broad distance peaks in DEER experiments.[56] A bifunctional label, attached to the protein at two introduced cysteines, can provide significant narrowing of the distance distribution due to a more rigid label attachment.[56−58] However, double-site attachment requires careful selection of the cysteine locations and some trial and error to avoid strain and adverse structural effects. For placement on an α-helix, two cysteines spaced at i and i+3, or i and i+4, have been successful,[56,59] but manual structural modeling becomes important for label placement at a nonhelical location. A number of attempts were made to place a pair of bifunctional spin-labels at positions appropriate to measure the open-to-closed conversion. A bifunctional site near the fixed position 48, which does not move during the conformational change, was paired with a site on either the F or G helices. Figure 5 shows how two BSL labels are modeled onto either the F or G helices in silico, using YASARA energy minimization server to avoid steric clashes.[60] The expected distances between two labels for the open and closed forms are 31.3 and 27.7 Å for the F helix, and 45.7 and 39.0 Å for the G helix, respectively. Of eight such constructs, four gave inclusion bodies upon expression, while the other four were expressed and purified in good yield. Two of these were selected for further study based on yield, stability, and unperturbed spectroscopic properties after labeling. Each construct contains a bifunctional site at the fixed position N33C and S35C. For the F helix, an additional site at K178C and D182C was added and will be referred to as BSL-F and for the G helix, and E195C and A199C was used and referred to as BSL-G (see Table 1 and Figure 5). For each of these pairs, a monofunctional version was created so that bifunctional and monofunctional spin-labeling results at the same sites can be compared. These mutants are referred to as MTSL-F and MTSL-G and are also defined in Table 1. Each of these proteins have been expressed, purified and labeled with either MTSL or BSL as appropriate and the extent of labeling verified by ESI-MS (Figure S6 and Table S1). Camphor binding for each of these mutants, with and without spin-label attachment were measured by UV/vis spectroscopy. As shown in Figure 6, Figure S7, and Table 2, the affinities are similar to the P450cam-4S control in which surface accessible cysteines are

Table 1. P450cam Mutants Used for DEER Studies

position	notation	mutation sites[a]
F helix	MTSL-F	S35C, Y179C
	BSL-F	N33C, S35C, K178C, D182C
G helix	MTSL-G	S35C, E195C
	BSL-G	N33C, S35C, E195C, A199C

[a]All of the P450cam mutants include C58S, C85S, C136S, and C285S to remove surface cysteines.

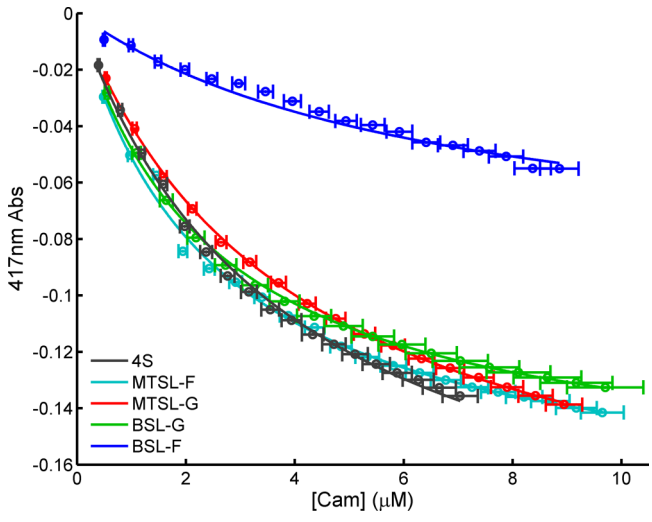

Figure 6. Camphor binding affinities of various P450cam mutants with spin-labels attached. Open circles are the raw data, and solid curves are the fitted binding curves.

DOI: 10.1021/jacs.6b04110
J. Am. Chem. Soc. 2016, 138, 10163−10172

Table 2. Camphor Binding Affinities for P450cam Mutants with and without Spin Labels

mutants	label	K_d (μM)[a]
4S	-	4.3(2)
MTSL-F	-	5.2(3)
	MTSL	2.3(1)
BSL-F	-	4.7(6)
	BSL	6.6(10)
MTSL-G	-	4.0(3)
	MTSL	3.8(1)
BSL-G	-	3.0(4)
	BSL	4.5(1)

[a]The fitted values for K_d correspond to 95% confidence interval.

removed, with the exception of the labeled form of BSL-F. For the bifunctional labeled form of this mutant, but not for the unlabeled or MTSL labeled forms, the camphor affinity is approximately 1.5-fold weaker, suggesting that BSL labeling on the F helix site is structurally disruptive. CW EPR spectra (Figures S8 and S9) and their g values (Table S2) for the labeled enzymes show that MTSL-G, BSL-G, and MTSL-F undergo the expected low- to high-spin conversion upon binding camphor. Subsequent binding of Pdx to these samples causes a partial conversion back to low-spin state with a shift in g_z from approximately 2.42 (Pdx-free) to 2.45 (Pdx-bound).[61,62] However, for BSL-F labeled with BSL, both the optical spectra (Figure S7) and EPR spectra (Figure S9D) suggest that the labeled form of this mutant is trapped in the open conformation.

DEER spectra for P450cam labeled with MTSL or BSL on either the F or G helices are compared in Figures 7 and 8. In each case, the BSL-labeled version shows DEER modulations that are better defined and extend to longer values of T (time delay following the primary spin echo) compared with the MTSL versions. For example, the BSL-G samples allow collection of useful DEER data to T values of 7.5 μs (Figure 7B), while the corresponding MTSL-G samples do not show DEER modulations beyond approximately 4 μs (Figure 7A). As a result, after Tikhonov regularization, the samples labeled with BSL show a dramatically narrowed distance distribution, allowing distances to be defined at much higher precision compared to the more mobile MTSL spin label (Table 3). For example, the fwhm for all peaks containing BSL-G pairs in Figure 8 is 2.3 Å compared to 10.1 Å for the MTSL-G distance

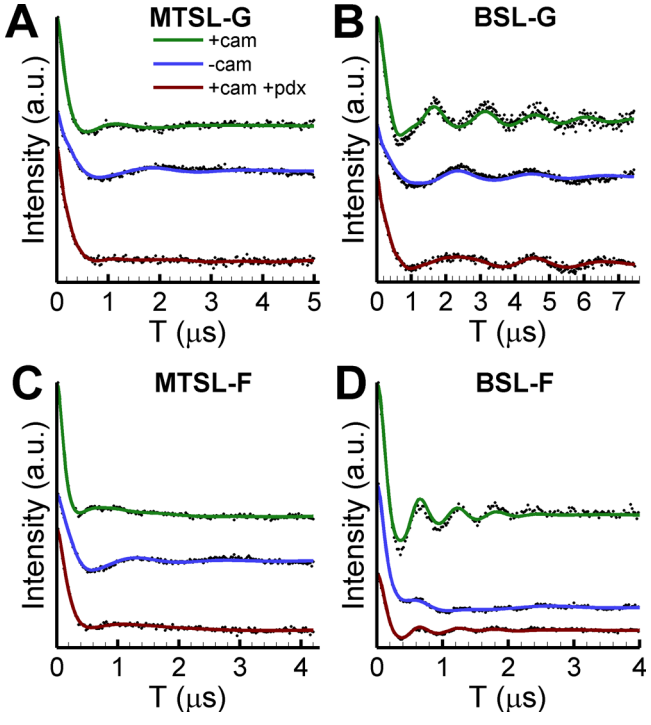

Figure 7. Time-domain DEER spectra of P450cam mutants with MTSL or BSL attached, as indicated. Camphor-bound (green), camphor-free (blue), and complex between Pdx and camphor-bound P450cam (red) are shown. Points are the raw data after background subtraction, and the solid traces are the fitted curves.

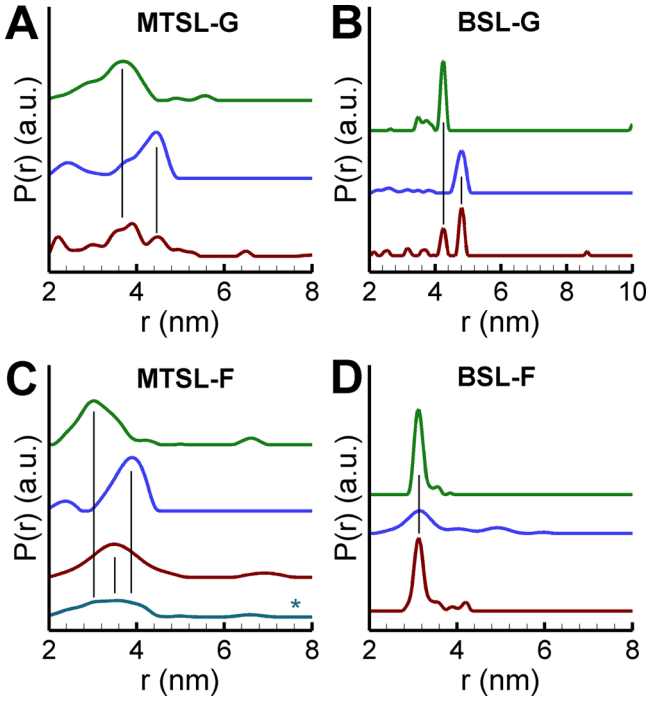

Figure 8. Distance distributions from DEER spectra of Figure 7. The distance distribution in C with an asterisk is the combination of 60% open and 40% closed distribution. The color scheme is identical to Figure 7.

Table 3. DEER Distances of P450cam Mutants in Different States (all DEER spectra are shown in Figures 7 and 8)

species	state	distance (Å)	Δd (Å)[a]	fwhm (Å)
MTSL-F	+cam	30.2	0	10.8
	-cam	38.8	8.6	8.6
	+cam + pdx	35.1	4.9	13.3
BSL-F	+cam	31.3	0	2.4
	-cam	31.3	0	7.0
	+cam + pdx	31.4	0.1	2.6
MTSL-G	+cam	36.8	0	12.8
	-cam	44.6	7.8	7.4
	+cam + pdx	39.0	2.2	-
BSL-G	+cam	42.6	0	1.9
	-cam	48.1	5.5	3.3
	+cam + pdx	42.6	0	2.0
		48.1	5.5	2.0

[a]The difference between each distance and the distance with camphor of each mutant.

DOI: 10.1021/jacs.6b04110
J. Am. Chem. Soc. 2016, 138, 10163−10172

pairs. The mode of labeling also affects the extent of movement as measured from the F or G helix during the open-to-closed transition. For MTSL-F, the distance between labels decreases by 8.6 Å when the open substrate−free enzyme is converted to the closed substrate bound state, while for MTSL-G, the distance decreases by 7.8 Å upon substrate binding. These values are in excellent agreement with the earlier study in which MTSL is used to measure a 8 Å movement of the tip of the loop (residue 190) between the F and G helices. For BSL-G, substrate binding causes a decrease in spin-label distance of 5.5 Å, somewhat less than the 8 Å movement observed with MTSL.[43] However, the decreased distribution widths of the BSL labeled forms clearly show that substrate binding induces a complete shift from one conformation at 48.1 Å to another at 42.6 Å, with no indication of a mixture of states. However, for BSL-F, no significant distance shift is observed upon substrate binding, indicating that BSL placed on the F helix abolishes the open-to-closed transition. In addition, there is a significant difference in the distribution widths, with the substrate-free form having a fwhm of 7.0 Å compared to 2.6 Å for the substrate-bound form. Thus, even though the average distance does not change for this labeled form, camphor still induces a reduced conformational heterogeneity in the position of the F helix.[63]

The effect of Pdx binding on the proteins labeled with MTSL or BSL on the individual F or G helices was investigated. As shown in Figures 7A and 8A, Pdx binding to MTSL-G labeled substrate-bound P450cam gives multiple broad peaks in the distance distribution plot, which roughly correspond to the distances observed for this labeled version in the open and closed conformations. This suggests that the protein may be adopting a mixture of open and closed states in response to Pdx binding. For MTSL-F, binding of Pdx to the substrate-bound enzyme shows a single broad peak (Figures 7C and 8C) at a distance of 35.1 Å, approximately midway between the closed and open states. Due to the width of these distributions it is not clear if the protein is adopting a single intermediate conformation or is instead converted into a mixture of the open and closed states. For example, shown in Figure 8C (distance distribution denoted with an asterisk) is the linear combination of 60% open and 40% closed distance distribution curves overlaid on the Pdx-bound distribution, showing that this mixture of the two states can reasonably account for the observed distribution. The Pdx-bound form of the substrate-bound BSL-G sample (Figures 7B and 8B) shows two peaks at precisely the distances as observed in the substrate-bound and substrate-free samples. The relative amplitudes of the two peaks are 63% open and 37% closed, suggesting that Pdx induces the closed conformation of BSL-G to convert to a mixture of open and closed conformations. Finally, the sample of substrate-bound BSL-F shows almost no response to the addition of Pdx (Figures 7D and 8D), suggesting that BSL labeling of the enzyme on the F helix abolishes the conformational change normally induced by camphor or Pdx.

Substrate Binding to the Open Conformation. Our DEER data suggest that Pdx induces conversion of P450cam to the open conformation even in the presence of camphor, while the g_z value for the low-spin signal in the presence of Pdx and camphor is distinct from that of the substrate-free open conformation. This suggests that camphor may have a unique interaction with the open conformation of the enzyme. In addition, to examine whether P450cam, after being crystallized in the open conformation, is able to resist conformational change due to camphor binding, we have determined the crystal structure at 1.5 Å resolution for the open form of the enzyme after soaking crystals in 2 mM camphor. The protein structure is essentially identical to the previously reported open substrate-free enzyme, with well-resolved electron density except for the region surrounding the B′ helix which is disordered in the fully open conformation.[41] A poorly resolved electron density feature is observed above the distal heme face near the camphor binding site (Figure 9). The density is roughly the correct size to be represented by a molecule of camphor, but its orientation is uncertain and is modeled in the structure in two alternate conformations, neither of which represents the orientation of camphor in the closed conformation. In addition, a water molecule is clearly observed bound to the iron on the distal heme face. It is clear that the enzyme crystallized in the open conformation resists conversion to the closed state upon soaking in camphor, presumably due to the effects of crystal contacts.

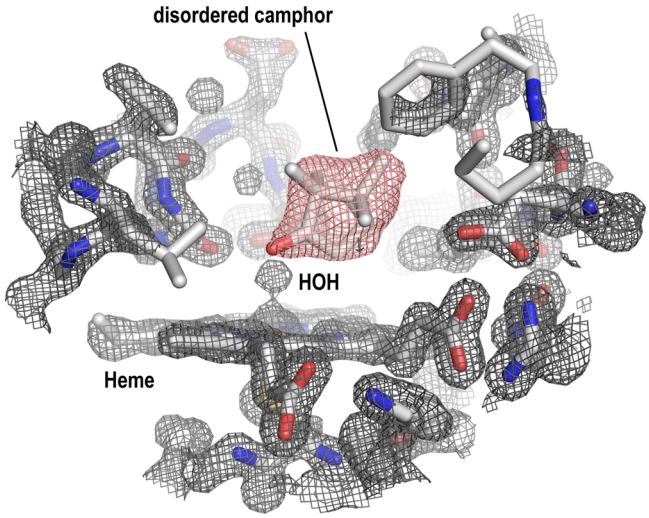

Figure 9. Crystal structure at 1.5 Å resolution of the open state of P450cam after soaking crystals in 2 mM camphor. Electron density is shown for the protein (black) at 2σ and for camphor (red) at 0.5σ. The disordered camphor is modeled into the density in one of two possible conformations reported in the PDB file (PDB number 5IK1). Figure was plotted by PyMol.

DISCUSSION

Substrate Binding to the Open Conformation. The observation of disordered substrate binding within the active-site channel of open-state P450cam has two important implications relevant to the current study. Even at the high (2 mM) concentrations of camphor used to soak open-state crystals, the electron density for camphor appears disordered and cannot be fitted well in any single orientation. In addition, electron density for the Tyr-96 side chain, which provides a hydrogen bond to camphor in the closed state, remained disordered as found in the substrate-free structure.[41] This shows that the open state of the substrate channel retains a general nonspecific affinity for camphor, but when it is prevented from closing, the orientation of substrate remains significantly disordered. The g_z value for the low-spin water-bound heme in the presence of both camphor and Pdx_{ox} is slightly different from the g_z value in the absence of both camphor and Pdx_{ox} because while both enzymes are in the open

DOI: 10.1021/jacs.6b04110
J. Am. Chem. Soc. 2016, 138, 10163−10172

state, the disordered camphor seen in our crystal structure may be expected to perturb the electronic structure and thus the *g* values (Figure S8). Finally, the inability of camphor binding to cause closure when soaked into open-state crystals clearly indicates that crystal contacts can resist conformational conversion in this enzyme and thus presents a complicating factor in reporting on this equilibrium.

Effects of Label Site and Type. Previous DEER studies of P450cam have utilized a monofunctional label at the tip of the loop between the F and G helix and have indicated that the states observed upon camphor and/or Pdx binding involve conversion between the fully open and fully closed states.[43,46] The current study examines the effect of placing both monofunctional and bifunctional labels onto either the F or G helix to examine effects of label type and placement. When the MTSL monofunctional label is placed on either the F or G helix, the camphor-induced shift causes a movement which is completely consistent with that observed when probed by DEER at the tip of the loop, or when observed by crystallography.[41,43] This result clearly indicates that in solution, substrate binding causes a concerted movement of both the F and G helices as a fixed unit from the fully open to the closed conformation. When the F or G helix is labeled with a bifunctional spin-label, the DEER modulations are greatly extended in the time domain and give significantly narrower distance distributions as a result of lower dispersion in rotamer sampling. This allows a greater precision in distance determination. Bifunctional label placement also has various effects on the extent of the conformational conversion. When placed on the G helix, at the same residues previously used for the lanthanide labeled NMR study, the enzyme undergoes a complete conversion from an open to a closed conformation upon camphor binding (Figure 8B), although the shift in distance (5.5 Å) is less than that observed for the monofunctional label. However, when the bifunctional label is installed on the F helix, the shift in the average distance upon substrate binding is completely abolished, while a significant difference in the distance distribution width is observed (Figures 7D and 8D). This suggests that shifts in the F/G structural equilibrium can be significantly affected by placement position for labels that have restricted rotamer conformations. Indeed, as indicated in Figure 5, model building for the bifunctional label placed on the F helix suggests potential steric interactions with the adjacent protein structure near the E and I helix. CW EPR spectra (Figure S9D) for the BSL-F enzyme shows no high-spin signal in either the substrate-free or camphor-bound states, suggesting that it is locked in the open conformation. This is supported by the observation that camphor binding to BSL-F is significantly weakened but not abolished (Figure 6). Finally, we have also examined the effects of an alternative placement of BSL on the F helix, at Y179C/Q183C, and find that the DEER derived distance of 37 Å is not dependent on the presence or absence of camphor (data not shown). This suggests that it is the placement of the bifunctional tether within the F helix, rather than disruption of a particular interaction, that is responsible for this effect. These results also suggest that the previous NMR study using a large bifunctional lanthanide label within the G helix may exhibit an altered conformational conversion of the protein. Indeed, the authors noted that substrate free P450cam labeled on the G helix with CLaNP-7 is unstable, suggesting that labeling has affected the protein structure.[48]

Effects of Pdx on P450cam Conformation. The use of multiple placements and types of spin-label on P450cam has afforded a more complete picture of the effects of Pdx binding on the ferric enzyme. When Pdx_{ox} is bound to MTSL-G labeled enzyme, multiple peaks are observed in the distance distribution that correspond roughly to the distances seen for the open and closed conformations (Figure 8A). The large distance distribution widths preclude a definitive conclusion to be made about whether Pdx bound to MTSL-G consists of a mixture of open and closed states or an intermediate conformation. However, for BSL-G, the significantly narrower distance distribution width allows observation that Pdx_{ox} binding induces a mixture of two states with distance peaks corresponding precisely to those of the open and closed conformations with no indication of an intermediate state. While it is not possible to make definitive quantitative conclusion about the relative contributions of states, the peak amplitude for the closed and open distance peaks in the presence of Pdx is approximately 40:60 respectively. When Pdx_{ox} is bound to MTSL-F, a broad distance distribution is observed with a peak that is intermediate between that of closed and open states. While it is unclear if this represents an intermediate distance or a mixture of open and closed states, Figure 8C suggests that a 40:60 mixture of the closed and open distance profiles provides an adequate agreement with the observed distance distribution. Thus, while labeling within the F or G helix may modulate the extent of the closed to open transition upon binding Pdx, it appears that the effects of Pdx binding reflect a shift in equilibrium between completely closed and open states rather than inducing an intermediate conformation. This provides support for a previous proposal that the structural states of this enzyme are controlled by conformational selection rather that induced fit.[40,64]

Effects of Redox State and Heme Coordination on the Pdx-Induced Conformational Shift. The DEER measurements reported here on the P450cam($Fe^{2+}CO{\cdot}S$)/Pdx_{ox} mixed oxidation state clearly show that Pdx_{ox} binding to substrate-bound ferrous-CO P450cam leave the enzyme in the closed conformation. This is in stark contrast with the effect of Pdx_{ox} on the ferric enzyme which shows conversion to the open state. These results strongly suggest that Pdx_{ox} and perhaps also Pdx_{red} exhibit a preference for binding to the open conformation of the enzyme. They also suggest that the ferrous-CO complex of the enzyme overrides the normal effector function of Pdx. It is known that CO bound to ferrous P450cam makes interactions with the distal heme cavity that are distinct from those of O_2 and presumably also the hydroperoxo complex.[52] We thus propose that these ligands, unlike CO, may allow Pdx to trigger the opening of the active site channel.

Conclusions. This study has used spin-labeling and DEER spectroscopy to investigate the conformational effect of Pdx on P450cam. Three main conclusions are drawn. First, the effector role of Pdx_{ox} binding to substrate-bound P450cam is to cause conversion from the closed to the open conformation. This effector role may also operate for the reduced states containing Pdx_{red} and ferrous or ferrous-oxy P450cam, but it is inhibited by the binding of CO to ferrous P450cam. Second, both the F and G helix appear to move during the Pdx_{ox}-induced conformational change, with no evidence for the stable population of intermediate states. Bifunctional labeling on the F helix appears to be detrimental to the Pdx_{ox}-induced conformational change. Finally, crystals of the open conformation are observed to bind

DOI: 10.1021/jacs.6b04110
J. Am. Chem. Soc. 2016, 138, 10163−10172

camphor in a disordered fashion without inducing closure of the substrate channel. These results have helped to define the effector role of Pdx on P450cam function.

METHODS

Protein Expression and Purification. All mutants of P450cam were prepared by site-directed mutagenesis of P450cam-4S, containing four mutations (C58S, C85S, C136S, and C285S) to remove surface-accessible cysteines.[43] The procedure for protein purification was described previously[41] unless detailed below. Briefly, *E. coli* BL21-(DE3), transformed with pET-P450cam, was grown in 50 mL of LB broth containing 100 mg/mL ampicillin overnight at 37 °C, and 10 mL was used to inoculate each of 4× 1 L of LB/ampicillin cultures. Protein expression was induced with 0.4 mM isopropyl β-D-1-thiogalactopyranoside (IPTG) after the OD_{600} reached 0.5−0.6, and the culture was maintained for an additional 20−24 h at 30 °C with shaking. Cells were harvested and lysed using a French press, the crude lysate was clarified by centrifugation, loaded on a 70 mL DEAE-anion exchange column (DEAE Sepharose Fast Flow, GE Healthcare), and eluted with a salt gradient of 30−270 mM KCl in 840 mL, and the fractions with A_{417}/A_{280} > 0.6 were pooled. After concentration by ultrafiltration, the sample was further purified on a 1.8L bed volume Sephacryl S-200 gel-filtration column and the fractions with A_{417}/A_{280} > 1.4 were retained for later experiments. Camphor was maintained in all buffers at 1 mM during purification.

For Pdx expression, pET-Pdx was transformed into BL21 (DE3), grown in 17 × 100 mm culture tubes in LB broth and 100 mg/mL ampicillin for 8 h at 37 °C and used to inoculate expression cultures in TB (Terrific Broth) broth containing 100 mg/mL ampicillin. After growth at 37 °C for 12 h, cultures were induced with 0.4 mM IPTG, and the temperature was dropped to 30 °C for 24 h. Cell were resuspended in 100 mL of 50 mM potassium phosphate (pH = 7.5) before being lysed by a French Press. After centrifugation to remove the cell debris, the lysate was applied to a DEAE-anion exchange column and eluted as described above, the fractions with A_{412}/A_{280} > 0.1 were concentrated and loaded to a Sephacryl S-200 size exclusion column. The fractions with A_{412}/A_{280} > 0.48 were retained for later experiments.

Camphor Affinity of P450cam. Camphor was removed before titration by a two-step procedure as previously described[41] involving successive PD-10 (GE Healthcare) gel filtration columns in 20 mM Bis-Tris, pH = 7.5. Ultrafiltration (Amicon Ultra 0.5 mL filters, 30 kDa cutoff) was used to exchange the buffer to 50 mM Bis-Tris, 150 mM KCl, and pH = 7.5. Camphor-free P450cam, 2 mL at 3.5 μM, was titrated stepwise with 1 μL aliquots of 1 mM camphor at 25 °C, and spectra were collected with a HP 8453 UV/vis spectrophotometer and analyzed by Origin9.0Pro.

Spin-Labeling and DEER Sample Preparation. Prior to spin-label introduction onto P450cam, DTT, and camphor were removed using PD-10 gel filtration columns as previously described. Spin-labeling was performed using MTSL (1 -oxyl-2,2,5,5-tetramethyl-Δ^3-pyrroline-3-methyl)methanethiosulfonate) or BSL (1*H*-pyrrol-1-yloxy-2,5-dihydro-2,2,5,5-tetramethyl-3,4-bis[[(methylsulfonyl)thio]-methyl]-(9CI)) purchased from Toronto Research Chemicals, and 4MT (4-maleimido-2,2,6,6-tetramethyl-1-piperidinyloxy, or 4-maleimido-TEMPO) was purchased from Sigma. All spin-labels were dissolved in DMSO. A 150 μL solution of 150 μM P450cam was incubated for 10 min at room temperature with a 10-fold excess of spin-label. An ultrafiltration membrane (Amicon ultracentrifugation, 30 kDa cutoff) was used to achieve a 6 × 5-fold dilution with 99% D_2O, 50 mM Tris, pD = 7.6, in order to remove free spin-label and exchange the sample into D_2O buffer. For camphor-containing samples, the buffer also contained 2 mM camphor and 150 mM KCl. The extent of labeling was measured (Figure S6) by ESI-mass spectroscopy with an Agilent 1260/6120 series LC/MS (6000 V capillary voltage, 150 V fragmentation voltage). A 4.6 × 50 mm Poroshell C18 column (Agilent) with a gradient of 30%−80% acetonitrile in water containing 0.1% formic acid was used to remove salt from P450cam prior to ESI-MS. Final EPR samples contained P450cam at 100 μM, Pdx at 250 μM if applicable, and 30% d_8-glycerol as a cryogenic glassing agent and were loaded into a quartz tube (100 mm length, 1.1 mm I.D. and 1.6 mm O.D., VitroCom) and frozen in liquid nitrogen for EPR experiments.

P450cam ($Fe^{2+}CO{\cdot}S/Pdx_{ox}$) Mixed Oxidation State. The P450cam ($Fe^{2+}CO{\cdot}S/Pdx_{ox}$) mixed oxidation state was prepared by careful addition of 1 equiv of Pdx_{red} to ferric P450cam in the presence of CO. Dithionite cannot be used in these experiments due to nitroxide reduction, so the Pdx_{red} was generated using putidaredoxin reductase (Pdr) and NADH as described previously. P450 was first labeled with MTSL on residues 48 and 190 using the P450cam-(4S2C) mutant[43] (C58S, C85S, C136S, C285S, S48C, and S190C) (see Supporting Information) and exchanged into D_2O buffer as described above. Pdx and Pdr were separately exchanged into D_2O with 50 mM Tris, 150 mM KCl, and 2 mM camphor by ultrafiltration, and NADH stock solution was dissolved in the same buffer. The concentration of NADH was determined by absorption at 340 nm (DH-mini light source and flame spectrophotometer, Ocean Optics) in an anaerobic environment. Variable amounts of NADH were added to Pdx samples purged with CO. Samples containing P450cam, Pdr, and 30% d_8-glycerol mixture were purged with CO for 10 min prior to addition of a variable amount of the Pdx:NADH mixture. To optimize the yield of P450cam($Fe^{2+}CO{\cdot}S$)/Pdx_{ox}, samples containing various ratios of P450cam to Pdx_{red} were examined by cwEPR to verify the absence of both ferric P450cam and Pdx_{red}. The resulting final concentrations of P450cam, Pdx, and Pdr were 99.46 μM, 92.21 μM, and 2.3 μM, respectively, and contained 30% d_8-glycerol.

EPR and DEER Spectroscopy. Continuous-wave EPR measurements were performed at X-band (9.5 GHz) using an EleXsys E500 spectrometer with a superhigh Q resonator (ER4122SHQE). Measurements of high-spin and low-spin spectra were made at 15 K, 2 mW, and 50 K, 0.2 mW (unsaturated condition), respectively. Q-band DEER spectra were measured using a Bruker EN5107D2 Q-band EPR/ENDOR probe-head at 30 K, by applying a deadtime-free four-pulse sequence ($\pi^*/2 - \tau_1 - \pi^* - (\tau_1 + T) - \pi^{\#} - (\tau_2 - T) - \pi^* - \tau_2 -$ [echo]) with probe pulses (*) and pump pulse (#) as indicated and T was advanced in 20 ns steps. The probe pulse lengths were 16 and 32 ns for the $\pi/2$ and π pulse, respectively. The length of the π pulse at the pump frequency was determined by nutation experiment, usually at either 16 or 20 ns. The frequency difference between the pump and probe pulse was 80 MHz.[65] The length of τ_1 was adjusted to a maximum in the ^2H nuclear modulation envelope (600 ns). DeerAnalysis2013 was used to analyze DEER spectra.[53] After background subtraction, least-squares fit was performed using Tikhonov regulation with L-curve selection to suppress artifact peaks and oversmoothing (see Supporting Information).

X-ray Crystallography. Crystals of P450cam in the open state were grown in the absence of camphor. Camphor was removed from protein stock solutions by buffer exchange into 100 mM Bis-Tris, pH 6.5, by gel filtration through two sequential PD-10 columns (GE Healthcare). Crystals of P450cam were grown by sitting-drop vapor diffusion at 4 °C. Substrate-free crystals grew from 100 mM Bis-Tris, pH 6.5, and 12−22% polyethylene glycol 8000 with and without 200 mM KCl. The crystals were transferred to cryoprotectant buffer consisting of 100 mM Bis-Tris, pH 6.5, 12% polyethylene glycol 8000, and 25% polyethylene glycol 600 with and without 200 mM KCl. In order to soak camphor into the substrate-free crystal, 2 mM camphor was added to the cryoprotectant buffer, and the crystal was allowed to soak for 15−30 min at room temperature. Crystals were then mounted on nylon loops and flash frozen at 77 K. X-ray diffraction data were collected at 100 K using beamline 7-1 at the Stanford Synchrotron Radiation Laboratory. Data were processed by MOSFLM[66] and Scala,[67] and molecular replacement was conducted with Molrep[68] using the open form P450cam structure (PDB entries 3L61). Model fitting and refinement were conducted with Coot[69] and Refmac5,[70] respectively. The final models were validated using Procheck,[71] Sfcheck,[72] Molprobity,[73] and the PDB validation server. Statistics for data collection and refinement are listed in Table S3 of the Supporting Information. The structure was deposited to the RCSB (PDB number 5IK1).

DOI: 10.1021/jacs.6b04110
J. Am. Chem. Soc. 2016, 138, 10163−10172

■ ASSOCIATED CONTENT

Supporting Information

The Supporting Information is available free of charge on the ACS Publications website at DOI: 10.1021/jacs.6b04110.

ESI-MS spectra, X-ray crystallographic data, EPR and UV−vis spectra, and DEER data analysis details (PDF)
X-ray structural model (PDB)
CIF data (CIF)

■ AUTHOR INFORMATION

Corresponding Author

*dbgoodin@ucdavis.edu

Present Addresses

†Valitor Inc., 130 Stanley Hall, Berkeley, CA 94720.
‡Department of Pathology, University of Michigan School of Medicine, Ann Arbor, MI 48109.

Notes

The authors declare no competing financial interest.

■ ACKNOWLEDGMENTS

This work was supported by the NIH (GM41049). We thank the staff at the Stanford Synchrotron Radiation Lightsource, a national user facility operated by Stanford University on behalf of the U.S. Department of Energy, Office of Basic Energy Sciences, and supported by the National Institutes of Health, National Center for Research Resources, Biomedical Technology Program, and by the National Institute of General Medical Sciences. We thank the CalEPR center, Prof. R. David Britt, and Prof. Stephen Cramer for instrumental and technical support, and Dr. William Myers for sharing the MATLAB scripts. We thank Prof. Thomas Poulos and Lizhi Tao for useful advice and discussion. Molecular graphics and analyses were performed with PyMol (Schrödinger) or UCSF Chimera package. UCSF Chimera is developed by the Resource for Biocomputing, Visualization, and Informatics at the University of California, San Francisco (supported by NIGMS P41-GM103311).

■ REFERENCES

(1) Sono, M.; Roach, M. P.; Coulter, E. D.; Dawson, J. H. *Chem. Rev.* **1996**, *96*, 2841.
(2) Poulos, T. L. *Chem. Rev.* **2014**, *114*, 3919.
(3) Wrighton, S. A.; Stevens, J. C. *Crit. Rev. Toxicol.* **1992**, *22*, 1.
(4) Johnson, E. F.; Stout, C. D. *Biochem. Biophys. Res. Commun.* **2005**, *338*, 331.
(5) Domanski, T. L.; He, Y. A.; Harlow, G. R.; Halpert, J. R. *J. Pharmacol. Exp. Ther.* **2000**, *293*, 585.
(6) Annalora, A.; Bobrovnikova-Marjon, E.; Serda, R.; Lansing, L.; Chiu, M. L.; Pastuszyn, A.; Iyer, S.; Marcus, C. B.; Omdahl, J. L. *Arch. Biochem. Biophys.* **2004**, *425*, 133.
(7) Denisov, I. G.; Makris, T. M.; Sligar, S. G.; Schlichting, I. *Chem. Rev.* **2005**, *105*, 2253−2277.
(8) Nelson, D. R. *Hum. Genomics* **2009**, *4*, 59.
(9) Poulos, T. L.; Finzel, B. C.; Gunsalus, I. C.; Wagner, G. C.; Kraut, J. *J. Biol. Chem.* **1985**, *260*, 16122.
(10) Poulos, T. L.; Finzel, B. C.; Howard, A. J. *J. Mol. Biol.* **1987**, *195*, 687.
(11) Sevrioukova, I. F.; Poulos, T. L. *Arch. Biochem. Biophys.* **2011**, *507*, 66.
(12) Tyson, C. A.; Lipscomb, J. D.; Gunsalus, I. C. *J. Biol. Chem.* **1972**, *247*, 5777.
(13) Sevrioukova, I. F.; Garcia, C.; Li, H.; Bhaskar, B.; Poulos, T. L. *J. Mol. Biol.* **2003**, *333*, 377.
(14) Griffin, B. W.; Peterson, J. A. *Biochemistry* **1972**, *11*, 4740.
(15) Fisher, M. T.; Sligar, S. G. *Biochemistry* **1987**, *26*, 4797.
(16) Davydov, R.; Macdonald, I. D. G.; Makris, T. M.; Sligar, S.; Hoffman, B. M. *J. Am. Chem. Soc.* **1999**, *121*, 10654.
(17) Schlichting, I.; Berendzen, J.; Chu, K.; Stock, A. M.; Maves, S. A.; Benson, D. E.; Sweet, R. M.; Ringe, D.; Petsko, G. A.; Sligar, S. G. *Science* **2000**, *287*, 1615.
(18) Macdonald, I. D. G.; Sligar, S. G.; Christian, J. F.; Unno, M.; Champion, P. M. *J. Am. Chem. Soc.* **1999**, *121*, 376.
(19) Nagano, S.; Poulos, T. L. *J. Biol. Chem.* **2005**, *280*, 31659.
(20) Spolitak, T.; Dawson, J. H.; Ballou, D. P. *J. Biol. Chem.* **2005**, *280*, 20300.
(21) Davydov, R.; Perera, R.; Jin, S.; Yang, T.-C.; Bryson, T. A.; Sono, M.; Dawson, J. H.; Hoffman, B. M. *J. Am. Chem. Soc.* **2005**, *127*, 1403.
(22) Rittle, J.; Green, M. T. *Science* **2010**, *330*, 933.
(23) Davydov, R.; Dawson, J. H.; Perera, R.; Hoffman, B. M. *Biochemistry* **2013**, *52*, 667.
(24) Lipscomb, J. D.; Sligar, S. G.; Namtvedt, M. J.; Gunsalus, I. C. *J. Biol. Chem.* **1976**, *251*, 1116.
(25) Shimada, H.; Nagano, S.; Hori, H.; Ishimura, Y. *J. Inorg. Biochem.* **2001**, *83*, 255.
(26) Pochapsky, S.; Pochapsky, T.; Wei, J. Y. *Biochemistry* **2003**, *42*, 5649.
(27) Tosha, T.; Yoshioka, S.; Takahashi, S.; Ishimori, K.; Shimada, H.; Morishima, I. *J. Biol. Chem.* **2003**, *278*, 39809.
(28) Wei, J. Y.; Pochapsky, T.; Pochapsky, S. *J. Am. Chem. Soc.* **2005**, *127*, 6974.
(29) Rui, R. L.; Pochapsky, S.; Pochapsky, T. *Biochemistry* **2006**, *45*, 3887.
(30) Zhang, W.; Pochapsky, S. S.; Pochapsky, T. C.; Jain, N. U. *J. Mol. Biol.* **2008**, *384*, 349.
(31) Poulos, T. L.; Howard, A. J. *Biochemistry* **1987**, *26*, 8165.
(32) Li, H.; Narasimhulu, S.; Havran, L. M.; Winkler, J. D.; Poulos, T. L. *J. Am. Chem. Soc.* **1995**, *117*, 6297.
(33) Ludemann, S. K.; Lounnas, V.; Wade, R. C. *J. Mol. Biol.* **2000**, *303*, 797.
(34) Pylypenko, O.; Schlichting, I. *Annu. Rev. Biochem.* **2004**, *73*, 991.
(35) Yao, H.; McCullough, C. R.; Costache, A. D.; Pullela, P. K.; Sem, D. S. *Proteins: Struct., Funct., Genet.* **2007**, *69*, 125.
(36) Dmochowski, I. J.; Crane, B. R.; Wilker, J. J.; Winkler, J. R.; Gray, H. B. *Proc. Natl. Acad. Sci. U. S. A.* **1999**, *96*, 12987.
(37) Dunn, A. R.; Dmochowski, I. J.; Bilwes, A. M.; Gray, H. B.; Crane, B. R. *Proc. Natl. Acad. Sci. U. S. A.* **2001**, *98*, 12420.
(38) Dunn, A. R.; Hays, A.-M. A.; Goodin, D. B.; Stout, C. D.; Chiu, R.; Winkler, J. R.; Gray, H. B. *J. Am. Chem. Soc.* **2002**, *124*, 10254.
(39) Hays, A.-M.; Dunn, A. R.; Chiu, R.; Gray, H. B.; Stout, C. D.; Goodin, D. B. *J. Mol. Biol.* **2004**, *344*, 455.
(40) Lee, Y. T.; Glazer, E. C.; Wilson, R. F.; Stout, C. D.; Goodin, D. B. *Biochemistry* **2011**, *50*, 693.
(41) Lee, Y. T.; Wilson, R. F.; Rupniewski, I.; Goodin, D. B. *Biochemistry* **2010**, *49*, 3412.
(42) Jeschke, G. *Annu. Rev. Phys. Chem.* **2012**, *63*, 419.
(43) Stoll, S.; Lee, Y. T.; Zhang, M.; Wilson, R.; Britt, R. D.; Goodin, D. B. *Proc. Natl. Acad. Sci. U. S. A.* **2012**, *109*, 12888.
(44) Hammes, G. G.; Chang, Y. C.; Oas, T. G. *Proc. Natl. Acad. Sci. U. S. A.* **2009**, *106*, 13737.
(45) Tripathi, S.; Li, H.; Poulos, T. L. *Science* **2013**, *340*, 1227.
(46) Myers, W. K.; Lee, Y. T.; Britt, R. D.; Goodin, D. B. *J. Am. Chem. Soc.* **2013**, *135*, 11732.
(47) Hiruma, Y.; Hass, M. A.; Kikui, Y.; Liu, W. M.; Olmez, B.; Skinner, S. P.; Blok, A.; Kloosterman, A.; Koteishi, H.; Lohr, F.; Schwalbe, H.; Nojiri, M.; Ubbink, M. *J. Mol. Biol.* **2013**, *425*, 4353.
(48) Skinner, S. P.; Liu, W. M.; Hiruma, Y.; Timmer, M.; Blok, A.; Hass, M. A.; Ubbink, M. *Proc. Natl. Acad. Sci. U. S. A.* **2015**, *112*, 9022.
(49) Hiruma, Y.; Gupta, A.; Kloosterman, A.; Olijve, C.; Olmez, B.; Hass, M. A.; Ubbink, M. *ChemBioChem* **2014**, *15*, 80.
(50) Hollingsworth, S. A.; Poulos, T. L. *Protein Sci.* **2015**, *24*, 49.
(51) Georgieva, E. R.; Roy, A. S.; Grigoryants, V. M.; Borbat, P. P.; Earle, K. A.; Scholes, C. P.; Freed, J. H. *J. Magn. Reson.* **2012**, *216*, 69.

DOI: 10.1021/jacs.6b04110
J. Am. Chem. Soc. 2016, 138, 10163−10172

(52) Spiro, T. G.; Soldatova, A. V.; Balakrishnan, G. *Coord. Chem. Rev.* **2013**, *257*, 511.
(53) Jeschke, G.; Chechik, V.; Ionita, P.; Godt, A.; Zimmermann, H.; Banham, J.; Timmel, C. R.; Hilger, D.; Jung, H. *Appl. Magn. Reson.* **2006**, *30*, 473.
(54) Galiano, L.; Blackburn, M. E.; Veloro, A. M.; Bonora, M.; Fanucci, G. E. *J. Phys. Chem. B* **2009**, *113*, 1673.
(55) Pettersen, E. F.; Goddard, T. D.; Huang, C. C.; Couch, G. S.; Greenblatt, D. M.; Meng, E. C.; Ferrin, T. E. *J. Comput. Chem.* **2004**, *25*, 1605.
(56) Fleissner, M. R.; Bridges, M. D.; Brooks, E. K.; Cascio, D.; Kalai, T.; Hideg, K.; Hubbell, W. L. *Proc. Natl. Acad. Sci. U. S. A.* **2011**, *108*, 16241.
(57) Hubbell, W. L.; Lopez, C. J.; Altenbach, C.; Yang, Z. *Curr. Opin. Struct. Biol.* **2013**, *23*, 725.
(58) Thompson, A. R.; Binder, B. P.; McCaffrey, J. E.; Svensson, B.; Thomas, D. D. *Methods Enzymol.* **2015**, *564*, 101.
(59) Sahu, I. D.; McCarrick, R. M.; Troxel, K. R.; Zhang, R.; Smith, H. J.; Dunagan, M. M.; Swartz, M. S.; Rajan, P. V.; Kroncke, B. M.; Sanders, C. R.; Lorigan, G. A. *Biochemistry* **2013**, *52*, 6627.
(60) Krieger, E.; Joo, K.; Lee, J.; Lee, J.; Raman, S.; Thompson, J.; Tyka, M.; Baker, D.; Karplus, K. *Proteins: Struct., Funct., Genet.* **2009**, *77* (S9), 114.
(61) Lipscomb, J. D. *Biochemistry* **1980**, *19*, 3590.
(62) Unno, M.; Christian, J. F.; Benson, D. E.; Gerber, N. C.; Sligar, S. G.; Champion, P. M. *J. Am. Chem. Soc.* **1997**, *119*, 6614.
(63) Lerch, M. T.; Yang, Z.; Brooks, E. K.; Hubbell, W. L. *Proc. Natl. Acad. Sci. U. S. A.* **2014**, *111*, E1201.
(64) Markwick, P. R.; Pierce, L. C.; Goodin, D. B.; McCammon, J. A. *J. Phys. Chem. Lett.* **2011**, *2*, 158.
(65) Polyhach, Y.; Bordignon, E.; Tschaggelar, R.; Gandra, S.; Godt, A.; Jeschke, G. *Phys. Chem. Chem. Phys.* **2012**, *14*, 10762.
(66) Leslie, A. G. W.; Powell, H. R. *Evolving Methods for Macromolecular Crystallography* **2007**, *245*, 41.
(67) Evans, P. R. *Proceedings of CCP4 Study Weekend* **1993**, 114.
(68) Vagin, A.; Teplyakov, A. *J. Appl. Crystallogr.* **1997**, *30*, 1022.
(69) Emsley, P.; Cowtan, K. *Acta Crystallogr., Sect. D: Biol. Crystallogr.* **2004**, *60*, 2126.
(70) Murshudov, G. N.; Vagin, A. A.; Dodson, E. J. *Acta Crystallogr., Sect. D: Biol. Crystallogr.* **1997**, *53*, 240.
(71) Laskowski, R. A.; MacArthur, M. W.; Moss, D. S.; Thornton, J. M. *J. Appl. Crystallogr.* **1993**, *26*, 283.
(72) Vaguine, A. A.; Richelle, J.; Wodak, S. J. *Acta Crystallogr., Sect. D: Biol. Crystallogr.* **1999**, *55*, 191.
(73) Lovell, S. C.; Davis, I. W.; Arendall, W. B.; de Bakker, P. I. W.; Word, J. M.; Prisant, M. G.; Richardson, J. S.; Richardson, D. C. *Proteins: Struct., Funct., Genet.* **2003**, *50*, 437.

DOI: 10.1021/jacs.6b04110
J. Am. Chem. Soc. 2016, 138, 10163−10172